Different spectroscopic behavior of coupled and freestanding monolayer graphene deposited by CVD on Cu foil

De Luca, Oreste; Grillo, Rossella; Castriota, Marco; Policicchio, Alfonso; De Santo, Maria Penelope; Desiderio, Giovanni; Fasanella, Angela; Agostino, Raffaele Giuseppe; Cazzanelli, Enzo; Giarola, Marco

Published in:
Applied Surface Science

DOI:
10.1016/j.apsusc.2018.07.064

Publication date:
2018

Applied Surface Science 458 (2018) 580–585

Contents lists available at ScienceDirect

Applied Surface Science

journal homepage: www.elsevier.com/locate/apsusc

Full Length Article

Different spectroscopic behavior of coupled and freestanding monolayer graphene deposited by CVD on Cu foil

Oreste De Luca[a,b,2], Rossella Grillo[a,c,1,2], Marco Castriota[a,b,*], Alfonso Policicchio[a,b,e], Maria Penelope De Santo[a], Giovanni Desiderio[b], Angela Fasanella[a], Raffaele Giuseppe Agostino[a,b,e], Enzo Cazzanelli[a,d,e], Marco Giarola[f], Gino Mariotto[f]

[a] Dipartimento di Fisica, Università della Calabria, Ponte P. Bucci, 87036, Cubo 31C, Arcavacata di Rende (CS), Italy
[b] Consiglio Nazionale delle Ricerche, Istituto di Nanotecnologia (Nanotec) – UoS Cosenza, Ponte P. Bucci, 87036, Cubo 31C, Arcavacata di Rende (CS), Italy
[c] Zernike Institute for Advanced Materials, University of Groningen, Nijenborgh 4, NL-9747AG Groningen, The Netherlands
[d] Notredame s.r.l., c/o Dipartimento di Fisica, Università della Calabria, Italy
[e] Consiglio Nazionale Interuniversitario Scienze Fisiche della Materia (C.N.I.S.M), Via della Vasca Navale, 84, 00146 Roma, Italy
[f] Dipartimento di Informatica, Università di Verona, Strada Le Grazie, 15, 37134 Verona, Italy

ARTICLE INFO

Keywords:
Graphene
Chemical vapor deposition
Copper foil
Raman spectroscopy

ABSTRACT

The growth of graphene on copper foil has been performed, following the well-known low-pressure chemical vapor (LP-CVD) procedure. The as-deposited monolayer graphene clearly exhibits two different coupling behaviors with the metal substrate, as demonstrated by visual microscopic investigation and by other experimental techniques, like Scanning Electron Microscopy (SEM) and micro-Raman spectroscopy. The single graphene sheet shows both large areas where it is coupled to the metal substrate and others where it exhibits freestanding-like characteristics. This phenomenology appears to be related to oxidation of the copper surface. In addition, we demonstrate the possibility to induce a variation of the coupling state by visible-light irradiation above a proper power threshold. The resulting change of the coupling with the metal substrate is associated to a local variation of the work function. Applications in high-performance electronic devices can be suitably tailored by optical methods and, in principle, by any local probe producing "hot spots" such as Scanning Tunneling Microscopy (STM) tips and electron beams.

1. Introduction

The experimental discovery of graphene [1,2] opened the doors to the world of nanomaterials. Thanks to its extraordinary properties, graphene and its derivatives will play a critical role in nanotechnology in the future across various technological domains [3]. A large number of techniques for the production of graphene were developed over the years, including epitaxial growth [4], mechanical [5], and chemical exfoliation [6] as well as chemical vapor deposition (CVD) [7–9]. Graphene grown on metal surfaces can interact strongly or weakly with the underlying substrate; in particular, a strong coupling is reported for Ru(0 0 0 1) [10], Rh(1 1 1) [11] and Ni [12] while a weak interaction involves Pt(1 1 1) [13], Ir(1 1 1) [4] and Cu [14,15] surfaces. The ability to synthetize high quality graphene on non-interacting substrates would allow to preserve the graphene's intrinsic properties, which is a fundamental prerequisite for graphene electronic devices (i.e. graphene directly deposited on a dielectric surface). Unfortunately, this route has not been developed yet. Direct growth of freestanding graphene on a surface would eliminate the transfer step on a nearly non-interacting substrate [16]. This last consolidate transfer procedure usually involves the PMMA/PVA methods to transfer graphene on the inert Si/SiO_2 surface [17,18]. A good alternative proposed to this purpose is to grow graphene directly on the metal oxides surfaces [19]. As reported by Gottardi et al. [20] high-quality monolayer graphene can be grown on a pre-oxidized Cu(1 1 1) surface, which is effectively decoupled from the underlying substrate (i.e. freestanding like). Another way to realize freestanding graphene is to grow it on metal surfaces and after to intercalate an oxygen layer in the graphene/metal interface. In fact, as reported by Voloshina et al. [21], the strong-coupled graphene/Ru(0 0 0 1) interface was successfully decoupled by the

* Corresponding author at: Dipartimento di Fisica, Università della Calabria, Ponte P. Bucci, 87036, Cubo 31C, Arcavacata di Rende (CS), Italy.
E-mail address: marco.castriota@fis.unical.it (M. Castriota).
[1] Present address: Département de Chimie Physique, Université de Genève, Quai Ernest-Ansermet 30, 1211 Genève, Switzerland.
[2] These authors contributed equally.

https://doi.org/10.1016/j.apsusc.2018.07.064
Received 30 April 2018; Received in revised form 30 June 2018; Accepted 10 July 2018
Available online 11 July 2018

intercalation of an oxygen layer.

Taking into account all these factors, in this work, monolayer graphene films were grown on copper (Cu) foil by the consolidate Chemical Vapor Deposition at low-pressure conditions (LP-CVD). The coexistence, in the resulting samples, of two kinds of coupling for monolayer graphene, is evidenced by optical and electronic microscopy as well as micro-Raman mapping. These two distinct regions will be labeled in the following as “coupled” and “freestanding-like” graphene, respectively, without strict correspondence to similar labels commonly used in the graphene literature. This phenomenon appears to be related to partial oxidation of the copper substrate. Moreover, the possibility to induce on a microscopic scale a transition from the “coupled” to the “freestanding-like” graphene via visible-light irradiation above a proper power threshold is evidenced. The resulting change of the coupling with the copper substrate is also associated to a localized work function variation. Applications in high-performance electronic devices can be suitably tailored by optical methods and, in principle, by any local probe producing “hot spots” such as STM tips and electron beams. In fact, such evidences open the doors to creation several graphene-based electronic devices, like gas sensors [22,23], solar cells [24,25], and field emitters [26].

2. Experimental section

2.1. Film deposition

The present graphene samples were grown on a thin copper foil (thickness 25 μm, 99.999% purity, ESPI Metals). The growth took place in a quartz-tube vacuum furnace where the base pressure was about 10^{-5} mbar [27]. The Cu surface was prepared by etching with H_2SO_4 0.25 M for 5 min and subsequently rinsed in milli-Q water. The samples were rinsed in ethanol and dried with argon, before being placed in the furnace. To avoid the formation of native oxide on the Cu surface, the samples were annealed at a temperature ranging between 907 and 977 °C in hydrogen flow (0.5 mbar). Subsequently, the samples were exposed to a mixture of hydrogen (0.5 mbar, MesserGas, purity 99.999%) and methane (0.5 mbar, MesserGas, purity 99.995%) for a time ranging between 2 and 4 min [15]. The samples were cooled down in argon atmosphere (99.999% purity, MesserGas, pressure 0.1 mbar) with an initial rate of 10 °C/min (in the range 927–477 °C) and, later, with a rate of 5 °C/minute (in the range 477–77 °C) [27].

2.2. Methods

A systematic characterization of different samples was carried out to investigate their structural, morphological and electronic properties, by Scanning Electron Microscopy (SEM) and Raman spectroscopy. SEM images were recorded by means of a Quanta FEG 400 (FEI) system. All of them were collected by using an electron beam of 15 keV over surface areas ranging from 25 μm^2 up to 250 μm^2 and magnification in the order of 10,000X. Micro-Raman spectra were collected by Horiba-Jobin Yvon apparatus, model LabRam HR, consisting of a single spectrograph equipped with: an objective 80X, a holographic grating (600 lines/mm) and a He-Ne laser (633 nm emission line). The maximum laser power flux impinging on the sample surface was about of 10^9 W/m^2: this power value was properly reduced by using neutral filters of optical density (OD) ranging from 0.3 up to 4.

3. Results and discussion

Fig. 1(a) shows a large-scale SEM image of graphene on Cu substrate where the copper grains are clearly visible on the surface. The different shades of gray that appear in this acquisition are quite similar and comparable in size to those shown in the Fig. 1(b), collected by an optical microscope.

Generally, in systems where graphene covers partially or entirely

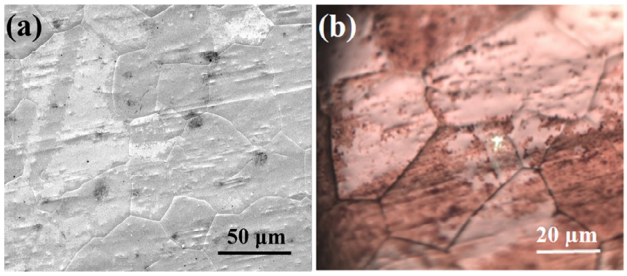

Fig. 1. (a) SEM image of graphene on Cu surface acquired on an area of about 210 × 180 μm^2. (b) Optical image collected by the microscope of the Raman apparatus, with the objective 80X. The area here represented is approximately 90 × 70 μm^2. The white spot in the center is the focus of the attenuated laser beam (OD4).

the whole surface, different shades of grey in SEM acquisitions can be observed. One possible explanation involves the different graphene film thickness [28–30]: lighter areas could correspond to graphene thin films (*e.g.* monolayer graphene) while darker regions could represent thicker depositions. Zhou et al. [29] clearly pointed out that secondary electron (SE) contrast of SEM acquisitions is strictly related to work function changes, depending on the number of graphene layers. In particular, they show that graphene work function rises as the thickness increases. However, other explanations are possible. Graphene work function also depends both on the chemical composition and morphology [13,31,32] of the substrate. Moreover, the specific crystalline surface [32] and the different orientation between graphene and substrate [33] can also influence the graphene work function. The lower work function, associated to the shinier areas, can also be explained in terms of variation of the graphene-to-metal surface distance. DFT calculations performed by Giovannetti et al. [34] show that the work function of the graphene layer on copper substrate shows an estimated shift of 0.55 eV by passing from the equilibrium separation (ca. 3.3 Å) to a larger distance (greater than 4.2 Å), when it assumes the free-standing-like value. This is due to the graphene/metal electron transfer resulting from the chemical interaction. In our case, as confirmed below by Raman analysis, the different shade of grey in SEM analysis, i.e. the local work function variation of graphene, is related to the different coupling between the single-layer graphene and the Cu surface. Color differences appear also to the optical microscope (see Fig. 1(b)), in similar way to previous observations made for ambient pressure CVD graphene on copper [35]. In the present case, comparable size of the “dark” and “bright” areas (10^3–10^4 μm^2) are observed. The regions preserving color and reflectivity of the clean Cu surface are labeled as “bright”. Conversely, the other areas appear brown colored, showing decreased reflectivity and are labeled “dark” regions. Taking into account the spatial resolution of micro-Raman analysis (~1 μm), adequate physical information can be gained on these two areas from the differences in their Raman spectra [36,37].

Two representative Raman spectra from these different regions are shown in Fig. 2. The spectra of the “bright” areas exhibit, in general, a very weak signal, but the intensity ratio between the G band and the 2D overtone is consistent with graphene monolayer formation [8,35–37]. This layer appears also highly ordered, being the D band absent or very weak. It is interesting to note that the G band falls at about 1600 cm^{-1}, a frequency value higher than usual [38,39]. When the G band exhibits this high frequency value, the 2D overtone is centered at about 2660 cm^{-1}. These evidences indicate an appreciable coupling between graphene and metal substrate. In the “dark” regions, on the contrary, all the Raman bands are stronger, while the intensity ratio 2D/G remarkably increases, being the shape of 2D band still well represented by a single mode curve. These findings are neither compatible with the formation of multilayer graphene having typical Bernal stacking [36,37] or with turbostratic multilayer [40]. Moreover, the G and the 2D bands shift to lower frequency, about 1572 cm^{-1} and 2630 cm^{-1},

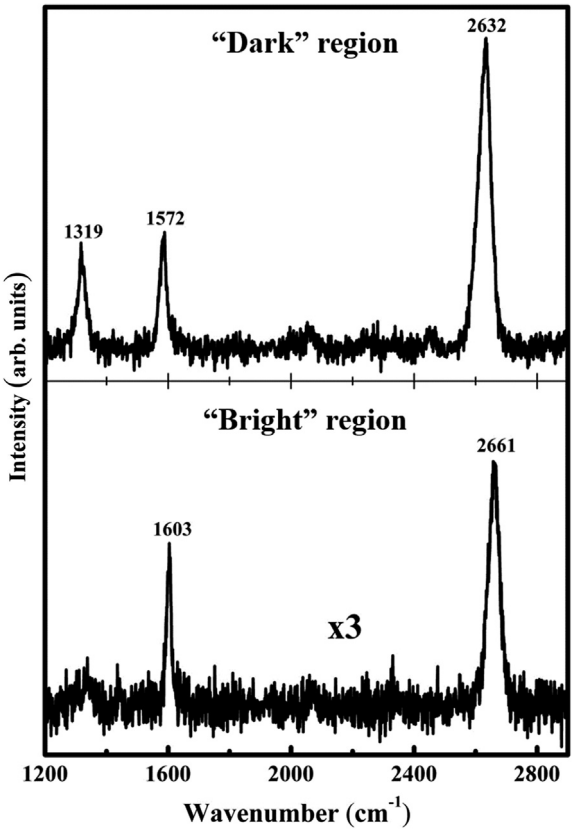

Fig. 2. Representative Raman spectra from optically appearing different regions of CVD graphene on copper foil, collected by the apparatus described in the text, with 633 nm excitation. The bottom spectrum is collected on a "bright" area, and is amplified by a factor 3 for comparison purposes with the top one, coming from a "dark" region.

respectively, which are typical of "freestanding-like graphene" [36,37,41]; finally, the rising of D band reveals some amount of disorder [42].

Summarizing, "bright" regions in optical images correspond to monolayer graphene in close contact with copper substrate, while the "dark" ones exhibit the spectroscopic characteristics of graphene more distant from the metal (see Fig. 2).

In order to gain further information, Raman measurements have been performed in the low frequency region of the spectra, to check the eventual occurrence of copper oxides, which has been found in previous works and related to the properties of graphene grown on copper [43–45].

These measurement reveals no significant peaks for the "bright" regions, while several Raman bands, assignable to Cu_2O [46–48] are found in all the "dark" areas. In particular, two sharp Raman peaks are clearly observed at 145 and 215 cm^{-1}, while other bands can be detected at 300, 360, 430, 525 and 645 cm^{-1}. Some of these minor features could be assigned to a minority occurrence of CuO compounds [46]. Being our main interest to correlate the oxide presence with the graphene properties, in Fig. 3 we show only the frequency range of the best evident peaks, comparing the "bright" and the "dark" regions of the samples.

The 145 cm^{-1} peak corresponds to an IR-active mode of T_{1u} symmetry, Raman-activated by the crystal disorder, while the 215 cm^{-1} is a strong second order overtone of a silent mode E_u, both characteristic of Cu_2O [46–48]. This finding, confirming the previous studies of Cermak [44] and Alvarez-Fraga [45], suggests that the decoupled configuration of monolayer graphene is associated to the oxidation of the copper substrate, which inhibits the graphene-metal electron exchange,

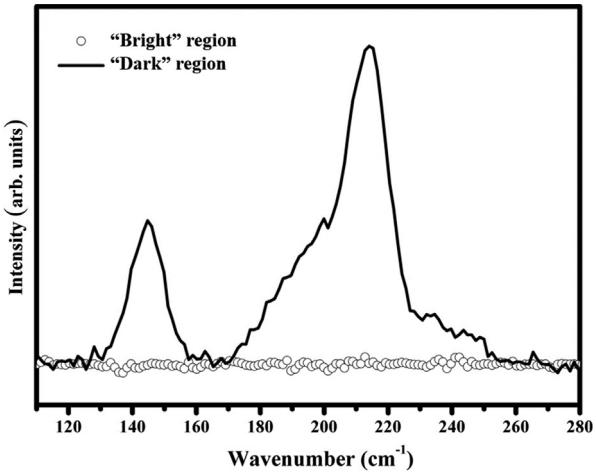

Fig. 3. Representative Raman spectra at the low frequency region from "bright" and "dark" regions of CVD graphene on copper foil. The spectrum collected on the "dark" region (solid line) shows two structures at about 145 cm^{-1} and 215 cm^{-1}, typical of Cu_2O. Conversely, Raman acquisition performed on the "bright" region (empty circles) does not show these Cu_2O bands.

inducing changes in the graphene work function.

To improve the understanding of such phenomena, an experiment has been performed to induce the transition from a "bright" a "dark" region, by a proper amount of laser irradiation. Raman spectra have been collected by using low laser power up to 25% of the full power, on a "bright" area, (Fig. 4(a) and (b)). The spectrum in Fig. 5(a), performed with a 25% laser power, shows the typical results: it indicates a well ordered graphene sheet (very weak D band) closely coupled to the copper substrate (very weak Raman signal in general), while the G band is peaked at 1605 cm^{-1} and the 2D overtone at 2664 cm^{-1}, typical of the bright regions (see Fig. 2). Another spectrum, collected from the same spot by using an increased laser power (50% of the full power for 600 s), is reported in Fig. 5(b), and exhibits some minor but interesting changes. The D band is peaked at 1331 cm^{-1}, the G band slightly downshifts from 1605 cm^{-1} to 1599 cm^{-1} and the 2D overtone from 2664 cm^{-1} to 2658 cm^{-1}, while the intensity ratio 2D/G does not change appreciably. These variations could be explained even as a

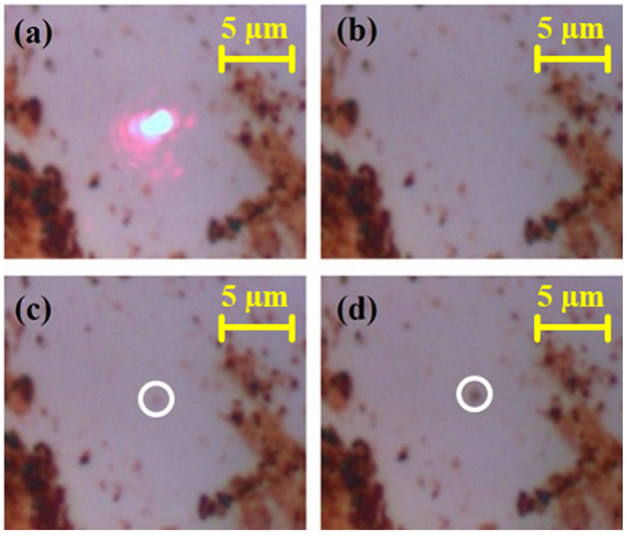

Fig. 4. (a) Strongly attenuated laser beam pointing out the irradiated spot. (b) Same image of graphene surface without laser beam: observe the bright coloration. (c) First small change in coloration (see white circle) after increased laser irradiation (50% full power). (d) Final greater change after full power irradiation (see white circle).

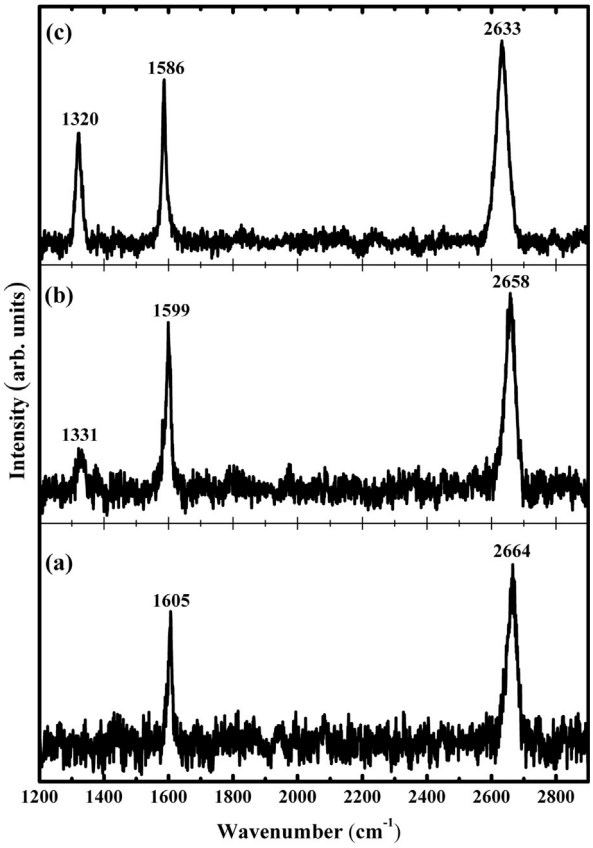

Fig. 5. Spectral evolution of the laser irradiated spot (the intensity scale has been properly adjusted for easy comparison of the three spectra): (a) First spectrum, collected e low intensity (25% of the full power). (b) Second spectrum, collected with higher laser power (50% of the full power). (c) Spectrum collected with low intensity, but after irradiation at full power.

simple thermal effect of the increased laser power. It is interesting to note a very little change of the color for the irradiated spot, after exposure to this higher laser power (Fig. 4(c)). Finally, the same spot was exposed to the full power of the laser source for 600 s. This treatment induced a stronger and irreversible change of the color (Fig. 4(d)), clearly related to a different interaction with the substrate. A new spectrum is collected from that spot, after the strong irradiation, in the same "non-perturbative" conditions of the first spectrum (25% full laser power): it reveals appreciable spectral changes (see Fig. 5(c)).

The D band increases in intensity, and downshifts to 1320 cm^{-1}; the G band downshifts to 1586 cm^{-1} and the 2D overtone is now at 2633 cm^{-1}, typical values of the "dark" regions. Moreover, the Raman signal is generally higher, as revealed by the increased signal to noise ratio. In fact, the intensity ratio 2D/G shows an appreciable increase, confirming once again that such Raman spectrum is due to a graphene monolayer region and not to a turbostratic multilayer accumulation [40], which is, in any case, very difficult to invoke as explanation of those changes, because only a local thermal treatment in air has been performed on the sample. Furthermore, the shape of the 2D band still corresponds to single-layer graphene rather than bilayer and few-layers ones [49–51]. Clearly all these changes cannot be due to a thermal effect during the measurement, because we are using the same low power of the first spectrum shown in Fig. 5(a). Another possible explanation for the spectral modifications could be, in principle, a thermal oxidation for the pure graphene monolayer under the previous strong laser irradiation. However, a previous study [52], carried out to obtain purposely the oxidation by thermal treatment of exfoliated 1-L graphene on Si/SiO_2, shows a quite different evolution of the Raman spectral parameters. In fact, the frequencies of G band as well as those of the 2D overtone were remarkably up-shifted upon graphene thermal oxidation, while in our case we observe the opposite trend. Another experiment [53] investigated the evolution of monolayer graphene, deposited on insulating substrate Si/SiO_2, under laser irradiation, for impinging powers comparable to those employed in Raman measurements. Once again, the resulting changes of the Raman bands do not correspond to our results. In that case, the G band frequency appears insensitive to the laser irradiation, while in our study we observe a remarkable softening.

In summary, we suggest that our observed Raman spectral changes are mainly due to a separation of the graphene single layer from the pure metal substrate, because of the growth of a metal oxide layer in between, favored probably by the thermal effect of laser irradiation.

As a final result, we can state that a proper laser irradiation can modify the strength of the metal-graphene electronic interaction, which characterize the two main configurations occurring spontaneously in our CVD samples after the cooling. This switch between different configurations is also associated to different optical properties in reflection, generating the apparent color change before and after laser irradiation (Fig. 4d). In fact, the deposition of a graphene monolayer in the metal-coupled configuration do not change appreciably the Cu reflectivity, at least in the visible range, so that these bright regions appear to the visual microscopic analysis as almost identical to the naked copper surface. In the dark regions, on the contrary, the graphene layer is less coupled to the metal substrate, because of the oxide layer grown in between, and the resulting reflectivity is lower. The weak Raman signals in the "bright" regions are ascribed to the anti-resonance effect of the strong coupling substrate-graphene, observed on several metals and leading to the total cancellation in some case, like Ni [54]. In this configuration, the graphene layer undergoes also to a compressive stress and the Raman bands frequencies result higher than in "dark" regions, which can be considered more similar to the freestanding case [55]. In this latter case, the Raman intensity is higher and the frequencies are closer to the values found for mechanically exfoliated samples. In fact, it is well known that graphene layers grown by CVD on strongly interacting metals, like Ni, cannot be observed by Raman spectroscopy when deposited on the metal, but can give a good Raman signal after removal from metal substrate and deposition on $Si\text{-}SiO_2$ [56]. In the case of metals not so strongly interacting, Raman spectra of graphene were observable both on the metal and after detachment [57], and the spectral differences between these two configurations are comparable to those observed in the present work between "dark" and "bright" regions.

The investigation of the effect of strong laser irradiation confirms such hypothesis. The connection between the laser-induced local heating and the oxidation of copper surface, which causes the graphene detachment from the substrate, can be due, in principle, to different mechanisms: either an intercalation of atmospheric oxygen, associated with some fracture of the hexagonal carbon network, which penetrates below the carbon layer and reacts with the copper, or a thermally activated migration of the oxygen present in the copper well below the surface [45]. The observed increase of D band intensity is a specific evidence for carbon bond breaking. Further laser irradiation experiments, followed by micro-Raman analysis, have been performed, to get additional data useful to determine the prevalent oxidation mechanism. The increase of D band intensity, indicating some damage of graphene network, has been always observed, while the formation of copper oxide can be not detected in some case. This finding suggest that copper oxidation is mainly due to thermal activated diffusion of the oxygen coming from below the surface, where it can be present in variable concentration. The Raman spectral patterns after this irreversible event become more similar to those of non-interacting graphene. Similar effects, due to copper surface oxidation, occurs, within a much longer time scale, in the deposited samples after CVD process, generating the many "dark" regions observed in this work, without strong laser irradiation. Based on our hypothesis we can expect also to find sometimes-

such “detached spots”, giving good Raman signal, in CVD deposited graphene on other metals, even in the case of strong coupling metals.

4. Conclusions

The deposition method used for the present work provides samples where a monolayer of graphene is roughly divided in two fractions, comparable for surface extension: regions with tight adhesion of carbon network to the metal and areas where the graphene layer is not in close contact with metallic copper.

An evolution from the metal-coupled graphene configuration to the one detached from the metal can be induced by a proper amount of laser irradiation, overcoming some power threshold. Further investigation can be necessary to better investigate this phenomenon, which appears quite promising for the development of many possible applications, with regard to the chemical interaction of copper surface and oxygen. In fact, we point out that the exposure to a suitable laser flux could allow to “write” paths of freestanding-like graphene on a coupled graphene layer modulating in this way both its optical response and the local work function. This could pave the way to a tailored manipulation of the electro-optical response over large areas such those needed for the control of the electron emission from graphene in thermionic energy converter (TIC) [58], electro-catalytic devices [59], graphene-based plasmonic systems [60] and many others fields.

Acknowledgment

This research was supported by the EOMAT PON03PE_00092_1 project and by POR CALABRIA FESR-FSE 2014-2020 – ASSE I – O. S. 1.2 Azione 1.2.2 Project: “MERAVIGLIE”.

Graphene samples were synthetized at Zernike Institute for Advanced Materials, University of Groningen (The Netherlands). The authors would like to thanks Prof. Petra Rudolf and Dr. Luca Bignardi for their kind hospitality and useful discussions.

References

[1] K.S. Novoselov, A.K. Geim, S.V. Morozov, D. Jiang, Y. Zhang, S.V. Dubonos, I.V. Grigorieva, A.A. Firsov, Electric field effect in atomically thin carbon films, Science 306 (2004) 666–669.
[2] K.S. Novoselov, D. Jiang, F. Schedin, T.J. Booth, V.V. Khotkevich, S.V. Morozov, A.K. Geim, Two-dimensional atomic crystals, Proc. Natl. Acad. Sci. USA 102 (2005) 10451–10453.
[3] S. Kumar, K. Chatterjee, Comprehensive review on the use of graphene-based substrates for regenerative medicine and biomedical devices, ACS Appl. Mater. Interf. 8 (2016) 26431–26457.
[4] J. Coraux, T.N. Plasa, C. Busse, T. Michely, Structure of epitaxial graphene on Ir (111), New J. Phys. 10 (2008) 043033.
[5] M. Yi, Z. Shen, A review on mechanical exfoliation for the scalable production of graphene, J. Mater. Chem. A 3 (2015) 11700–11715.
[6] K. Parvez, Z.S. Wu, R. Li, X.J. Liu, R. Graf, X. Feng, K. Müllen, Exfoliation of graphite into graphene in aqueous solutions of inorganic salts, J. Am. Chem. Soc. 136 (2014) 6083–6091.
[7] A. Reina, H. Son, L. Jiao, B. Fan, M.S. Dresselhaus, Z. Liu, J. Kong, Transferring and identification of single-and few-layer graphene on arbitrary substrates, J. Phys. Chem. C 112 (2008) 17741–17744.
[8] X. Li, W. Cai, J. An, S. Kim, J. Nah, D. Yang, R. Piner, A. Velamakanni, I. Jung, E. Tutuc, S.K. Banerjee, L. Colombo, R.S. Ruoff, Large-area synthesis of high-quality and uniform graphene films on copper foils, Science 324 (2009) 1312–1314.
[9] P. Avouris, C. Dimitrakopoulos, Graphene: synthesis and applications, Mater. Today 15 (2012) 86–97.
[10] P.W. Sutter, J.-I. Flege, E.A. Sutter, Epitaxial graphene on ruthenium, Nat. Mater. 7 (2008) 406–411.
[11] E.N. Voloshina, Yu.S. Dedkov, S. Torbrügge, A. Thissen, M. Fonin, Graphene on Rh (111): Scanning tunneling and atomic force microscopies studies, Appl. Phys. Lett. 100 (2012) 241606.
[12] A. Dahal, M. Batzill, Graphene–nickel interfaces: a review, Nanoscale 6 (2014) 2548–2562.
[13] P. Sutter, J.T. Sadowski, E. Sutter, Graphene on Pt (111): growth and substrate interaction, Phys. Rev. B 80 (2009) 245411.
[14] L. Gao, J.R. Guest, N.P. Guisinger, Epitaxial graphene on Cu (111), Nano Lett. 10 (2010) 3512–3516.
[15] C. Mattevi, H. Kim, M. Chhowalla, A review of chemical vapour deposition of graphene on copper, J. Mater. Chem. 21 (2011) 3324–3334.
[16] A.K. Geim, Graphene: status and prospects, Science 324 (2009) 1530–1534.
[17] X. Li, Y. Zhu, W. Cai, M. Borysiak, B. Han, D. Chen, R.D. Piner, L. Colombo, R.S. Ruoff, Transfer of large-area graphene films for high-performance transparent conductive electrodes, Nano Lett. 9 (2009) 4359–4363.
[18] H. Van Ngoc, Y. Qian, S.K. Han, D.J. Kang, PMMA-etching-free transfer of wafer-scale chemical vapor deposition two-dimensional atomic crystal by a water soluble polyvinyl alcohol polymer method, Sci. Rep. 6 (2016) 33096.
[19] M. Zabeti, W.M.A. Wan Daud, M.K. Aroua, Activity of solid catalysts for biodiesel production: a review, Fuel Process. Technol. 90 (2009) 770–777.
[20] S. Gottardi, K. Müller, L. Bignardi, J.C. Moreno-López, T.A. Pham, O. Ivashenko, M. Yablonskikh, A. Barinov, J. Björk, P. Rudolf, M. Stöhr, Comparing graphene growth on Cu (111) versus oxidized Cu (111), Nano Lett. 15 (2015) 917–922.
[21] E. Voloshina, N. Berdunov, Y. Dedkov, Restoring a nearly free-standing character of graphene on Ru (0001) by oxygen intercalation, Sci. Rep. 6 (2016) 20285.
[22] S.S. Varghese, S. Lonkar, K.K. Singh, S. Swaminathan, A. Abdala, Recent advances in graphene based gas sensors, Sens. Actuat. B Chem. 218 (2015) 160–183.
[23] Y. Seekaew, D. Phokharatkul, A. Wisitsoraat, C. Wongchoosuk, Highly sensitive and selective room-temperature NO_2 gas sensor based on bilayer transferred chemical vapor deposited graphene, Appl. Surf. Sci. 404 (2017) 357–363.
[24] X. Wang, L. Zhi, K. Müllen, Transparent, conductive graphene electrodes for dye-sensitized solar cells, Nano Lett. 8 (2008) 323–327.
[25] K. Lukaszkowicz, M. Szindler, A. Drygała, L.A. Dobrzański, M.P. vel Prokopowicz, I. Pasternak, A. Przewloka, M.M. Szindler, M. Domanski, Graphene-based layers deposited onto flexible substrates: used in dye-sensitized solar cells as counter electrodes, Appl. Surf. Sci. 424 (2017) 157–163.
[26] S. Kumar, G.S. Duesberg, R. Pratap, S. Raghavan, Graphene field emission devices, Appl. Phys. Lett. 105 (2014) 103107.
[27] L. Bignardi, W.F. van Dorp, S. Gottardi, O. Ivashenko, P. Dudin, A. Barinov, J.T.M. De Hosson, M. Stohr, P. Rudolf, Microscopic characterisation of suspended graphene grown by chemical vapour deposition, Nanoscale 5 (2013) 9057–9061.
[28] F. Yang, Y. Liu, W. Wu, W. Chen, L. Gao, J. Sun, A facile method to observe graphene growth on copper foil, Nanotechnology 23 (2012) 475705.
[29] Y. Zhou, D.S. Fox, P. Maguire, R. O'Connell, R. Masters, C. Rodenburg, H. Wu, M. Dapor, Y. Chen, H. Zhang, Quantitative secondary electron imaging for work function extraction at atomic level and layer identification of graphene, Sci. Reps. 6 (2016) 21045.
[30] H.D. Le, T.T.T. Ngo, D.Q. Le, X.N. Nguyen, N.M. Phan, Adv. Nat. Sci.: Nanosci. Nanotech. 4 (2013) 035012.
[31] E. Loginova, S. Nie, K. Thürmer, N.C. Bartelt, K.F. McCarty, Defects of graphene on Ir (111): Rotational domains and ridges, Phys. Rev. B 80 (2009) 85430.
[32] N. Srivastava, Q. Gao, M. Widom, R.M. Feenstra, S. Nie, K. McCarty, I. Vlassiouk, Low-energy electron reflectivity of graphene on copper and other substrates, Phys. Rev. B 87 (2013) 245414.
[33] Y. Murata, E. Starodub, B.B. Kappes, C.V. Ciobanu, N.C. Bartelt, K.F. McCarty, S. Kodambaka, Orientation-dependent work function of graphene on Pd (111), Appl. Phys. Letts. 97 (2010) 143114.
[34] G. Giovannetti, P.A. Khomyakov, G. Brocks, V.M. Karpan, J. van den Brink, P.J. Kelly, Doping graphene with metal contacts, Phys. Rev. Letts. 101 (2008) 026803.
[35] E. Cazzanelli, O. De Luca, D. Vuono, A. Policicchio, M. Castriota, G. Desiderio, M.P. De Santo, A. Aloise, A. Fasanella, T. Rugiero, R.G. Agostino, Characterization of graphene grown on copper foil by chemical vapor deposition (CVD) at ambient pressure conditions, J. Raman Spectr. 49 (2018) 1006–1014.
[36] A.C. Ferrari, J.C. Meyer, V. Scardaci, C. Casiraghi, M. Lazzeri, F. Mauri, S. Piscanec, D. Jiang, K.S. Novoselov, S. Roth, A.K. Geim, Raman spectrum of graphene and graphene layers, Phys. Rev. Letts. 97 (2006) 187401.
[37] L.M. Malard, M.A. Pimenta, G. Dresselhaus, M.S. Dresselhaus, Raman spectroscopy in graphene, Phys. Rep. 473 (2009) 51–87.
[38] A. Guermoune, T. Chari, F. Popescu, S.S. Sabri, J. Guillemette, H.S. Skulason, T. Szkopek, M. Siaj, Chemical vapor deposition synthesis of graphene on copper with methanol, ethanol, and propanol precursors, Carbon 49 (2011) 4204–4210.
[39] O. Frank, J. Vejpravova, V. Holy, L. Kavan, M. Kalbac, Interaction between graphene and copper substrate: the role of lattice orientation, Carbon 68 (2014) 440–451.
[40] D.R. Lenski, M.S. Fuhrer, Raman and optical characterization of multilayer turbostratic graphene grown via chemical vapor deposition, J. Appl. Phys. 110 (2011) 013720.
[41] M. Castriota, E. Cazzanelli, D. Pacilè, L. Papagno, C.O. Girit, J.C. Meyer, A. Zettl, M. Giarola, G. Mariotto, Spatial dependence of Raman frequencies in ordered and disordered monolayer graphene, Diam. Rel. Mater. 19 (2010) 608–613.
[42] A.C. Ferrari, Raman spectroscopy of graphene and graphite: disorder, electron–phonon coupling, doping and nonadiabatic effects, Solid State Commun. 143 (2007) 47–57.
[43] X. Yin, Y. Li, F. Ke, C. Lin, H. Zhao, L. Gan, Z. Luo, R. Zhao, T.F. Heinz, Z. Hu, Evolution of the Raman spectrum of graphene grown on copper upon oxidation of the substrate, Nano Res. 7 (2014) 1613–1622.
[44] J. Cermák, T. Yamada, K. Ganzerová, B. Rezek, Doping effects and grain boundaries in thermal CVD graphene on recrystallized Cu foil, Adv. Mater. Interf. 3 (2016) 1600166.
[45] L. Álvarez-Fraga, Juan Rubio-Zuazo, F. Jiménez-Villacorta, E. Climent-Pascual, R. Ramírez-Jiménez, C. Prieto, A. de Andrés, Oxidation mechanisms of copper under graphene: the role of oxygen encapsulation, Chem. Mater. 29 (2017) 3257–3264.
[46] L. Debbichi, M.C. Marco de Lucas, J.F. Pierson, P. Krüger, Vibrational properties of CuO and Cu_4O_3 from first-principles calculations, and Raman and infrared spectroscopy, J. Phys. Chem C 116 (2012) 10232–10237.

[47] T. Sander, C.T. Reindl, M. Giar, B. Eifert, M. Heinemann, C. Heiliger, P.J. Klar, Correlation of intrinsic point defects and the Raman modes of cuprous oxide, Phys. Rev. B 90 (2014) 045203.
[48] A. Singhal, M.R. Pai, R. Rao, K.T. Pillai, I. Lieberwirth, A.K. Tyagi, Copper (I) oxide nanocrystals–one step synthesis, characterization, formation mechanism, and photocatalytic properties, Eur. J. Inorg. Chem. 14 (2013) 2640–2651.
[49] V.N. Popov, 2D Raman band of single-layer and bilayer graphene, J. Phys.: Conf. Ser. 682 (2016) 012013.
[50] J.S. Park, A. Reina, R. Saito, J. Kong, G. Dresselhaus, M.S. Dresselhaus, G′ band Raman spectra of single, double and triple layer graphene, Carbon 47 (2009) 1303–1310.
[51] A.C. Ferrari, D.M. Basko, Raman spectroscopy as a versatile tool for studying the properties of graphene, Nat. Nanotech. 8 (2013) 235.
[52] S.P. Surwade, Z. Li, H. Liu, Thermal oxidation and unwrinkling of chemical vapor deposition-grown graphene, J. Phys. Chem. C 116 (2012) 20600–20606.
[53] G. Amato, G. Milano, U. Vignolo, E. Vittone, Kinetics of defect formation in chemically vapor deposited (CVD) graphene during laser irradiation: the case of Raman investigation, Nano Res. 8 (2015) 3972–3981.
[54] A. Allard, L. Wirtz, Graphene on metallic substrates: suppression of the Kohn anomalies in the phonon dispersion, Nano Lett. 10 (2010) 4335–4340.
[55] O. Frank, G. Tsoukleri, J. Parthenios, K. Papagelis, I. Riaz, R. Jalil, K.S. Novoselov, C. Galiotis, Compression behavior of single-layer graphenes, ACS Nano 4 (2010) 3131–3138.
[56] T.H. Bointon, M.D. Barnes, S. Russo, M.F. Craciun, High quality monolayer graphene synthesized by resistive heating cold wall chemical vapor deposition, Adv. Mater. 27 (2015) 4200–4206.
[57] W. Cai, R.D. Piner, Y. Zhu, X. Li, Z. Tan, H.C. Floresca, C. Yang, L. Lu, M.J. Kim, R.S. Ruoff, Synthesis of isotopically-labeled graphite films by cold-wall chemical vapor deposition and electronic properties of graphene obtained from such films, Nano Res. 2 (2009) 851.
[58] S.J. Liang, L.K. Ang, Electron thermionic emission from graphene and a thermionic energy converter, Phys. Rev. Appl. 3 (2015) 014002.
[59] Y. Yan, Q. Liu, X. Dong, N. Hao, S. Chen, T. You, H. Mao, K. Wang, Copper (I) oxide nanospheres decorated with graphene quantum dots display improved electrocatalytic activity for enhanced luminol electrochemiluminescence, Microchim. Acta 183 (2016) 1591–1599.
[60] L. De Sio, U. Cataldi, T. Bürgi, N. Tabiryan, T.J. Bunning, Control of the plasmonic resonance of a graphene coated plasmonic nanoparticle array combined with a nematic liquid crystal, AIP Adv. 6 (2016) 075114.